Physics Letters A ••• (••••) •••–•••

Contents lists available at ScienceDirect

Physics Letters A

www.elsevier.com/locate/pla

Enhancement of precision and reduction of measuring points in tomographic reconstructions

H. Lustfeld [a,*], J.A. Hirschfeld [a], M. Reißel [b], B. Steffen [c]

[a] IFF-1 Forschungszentrum Jülich, D52425 Jülich, Germany
[b] Fachhochschule Aachen, Abteilung Jülich, D52428 Jülich, Germany
[c] JSC Forschungszentrum Jülich, D52425 Jülich, Germany

ARTICLE INFO

Article history:
Received 19 May 2010
Received in revised form 11 November 2010
Accepted 7 January 2011
Available online xxxx
Communicated by A.P. Fordy

Keywords:
Inverse problems
Image reconstruction
Fuel cells

ABSTRACT

Accurate external measurements are required in tomographic problems to obtain a reasonable knowledge of the internal structures. Crucial is the distribution of the external measuring points. We suggest a procedure how to systematically optimize this distribution viz. to increase the precision (i.e. to shrink error bars) of the reconstruction by detecting the important and by eliminating the irrelevant measuring points. In a realistic numerical example we apply our scheme to magnetotomography of fuel cells. The result is striking: Starting from a smooth distribution of measuring points on a surface of a cuboid around the fuel cell, the number of measuring points can systematically be reduced by more than 90%. At the same time the precision increases by a factor of nearly 3.

1. Introduction

The task of any tomographic method consists in determining an internal structure by external measurements [1–3]. The internal structure can be a radioactive material [4] or a radioactive tracer in a biological body [5–7]. It can also be a distribution of specific conductivities [8–12] or electric current densities [13,14]. It is usually given by a (not necessarily continuous) function in space, but for the reconstruction a finite dimensional vector space V with dimension N_c (for example N_c voxels with constant properties in each) is selected and the structure is approximated by an unknown vector $\tilde{\mathbf{s}} \in V$.

The internal structure will give rise to an external signal. This signal can be "intrinsic". Examples are a radioactive tracer or electric current distributions in the brain or in a fuel cell. But the signal can also be a response to X-ray radiation [15], electric currents [9] injected into the system [11,16], magnetic fields, or other perturbations. Mathematically these can be expressed by a parameter set $\mathbf{p}$, describing the action on the internal structure.

The external signal can be measured at various positions defining a measurement vector $\tilde{\mathbf{m}}$ in a vector space $\hat{V}$ with dimension N_H, equal to the number of measuring points for scalar quantities. A unique transformation $\mathbf{A}$ exists, which maps the internal structure onto the external signal

$$\mathbf{A}(\tilde{\mathbf{s}}, \mathbf{p}) = \tilde{\mathbf{m}}. \tag{1}$$

Finding the inverse of the mapping $\mathbf{A}$ with respect to $\tilde{\mathbf{s}}$ defines the problem of tomographic reconstruction. To have a unique inverse, $N_H \geqslant N_c$ is required. $N_H \gg N_c$ is common and will be considered here. $N_H < N_c$ requires further information (e.g. maximal entropy solutions in MEG [17]).

There are various possibilities for optimizing the tomographic problem. Isaacson [8] suggests the optimization of $\mathbf{p}$ (in his case $\mathbf{p}$ were electrical currents injected into the structure) such that the response is optimum. Note that this optimization scheme depends strongly on the structure $\tilde{\mathbf{s}}$. A detailed description and application to the EIT problem is given in [9]. A different optimization scheme has been looked for in [18] with the intention that different measurements should be as independent as possible. Another new reconstruction algorithm for Radon data, based on polynomial optimization, has been developed [19,20] and applied [21]. An increase of the efficiency by a factor of 2 has been reported [20].

How the distribution of the measuring points can be systematically optimized in a tomographic problem will be dealt with in this Letter. Since in general the positions of measuring devices cannot be moved easily, this optimization must not depend on the structure $\tilde{\mathbf{s}}$ directly.

For simplicity we will assume here that the signal is either intrinsic or that the parameter set $\mathbf{p}$ is fixed. Then the tomographic problem can be tackled in the following iterative manner: 1) The problem is linearized around an operating point $\tilde{\mathbf{s}}_0$, 2) the linearized problem is solved with solution $\tilde{\mathbf{s}}_1$, and 3) this is inserted as the new operating point, around which the problem is linearized again, etc. However, the typical problems of tomography (an ill defined inverse of $\mathbf{A}$, the question of where to position

* Corresponding author.
E-mail address: h.lustfeld@fz-juelich.de (H. Lustfeld).

0375-9601/$ – see front matter
doi:10.1016/j.physleta.2011.01.015

the measuring devices) appear already in the first step and we restrict ourselves to the first linearization. It should also be mentioned i) the linearization around the operating point is quite often a very good approximation or even exact [18,22,23], ii) the methods described below could be applied in the same manner at each further iterative step.

Therefore there are good reasons to consider possible optimizations for the linear regime around an operating point. Novel equations detecting the optimum measuring points will be derived in the next section, in the subsequent section the power of these equations will be demonstrated by an example and a summary will be given in the conclusion.

It should be noted that for problems where constraints of the form [24] $\tilde{\mathbf{s}} \geqslant 0$ become essential our scheme cannot be applied directly. This will be discussed in a forthcoming article.

2. Derivation of the optimization equations

If the tomographic problem (1) is not linear from the outset an operating point has to be specified around which the equation will be linearized. This operating point is naturally chosen by previous knowledge about the system. E.g. in tomography of the brain [7] the normal distribution of tissue is a natural ansatz, whereas for a fuel cell [25] the current density distribution [26] of the faultless operation specifies an adequate operating point.

The linearized problem of (1) is formulated as follows:

$$\mathbf{m} = \mathcal{S}\mathbf{s}, \quad \mathcal{S} = \left.\frac{\partial \mathbf{A}}{\partial \tilde{\mathbf{s}}}\right|_{\tilde{\mathbf{s}}_0}, \ \mathbf{s} = \tilde{\mathbf{s}} - \tilde{\mathbf{s}}_0, \ \mathbf{m} = \tilde{\mathbf{m}} - \mathbf{A}(\tilde{\mathbf{s}}_0). \tag{2}$$

For tomographic problems of the type (2) we present in this Letter a distribution of measuring points that minimizes the errors when determining the internal structure $\mathbf{s}$.

The ith row of the matrix $\mathcal{S}$ corresponds to the measuring point $\mathbf{x}_i$ and to make this explicit we choose the notation $S_{\mathbf{x}_i,k}$ for the matrix elements. Since the number of row vectors of $\mathcal{S}$ is much larger than their dimension one could try to find an appropriate basis by eliminating vectors pointing essentially in the same direction as others [18,27]. However, this scheme has an important drawback: Information, essential for the high resolution portion of $\mathbf{s}$, generically gives small contributions to the measurements. Thus, even if two vectors $\mathbf{v}_{\mathbf{x}_i}$ and $\mathbf{v}_{\mathbf{x}_j}$ are nearly parallel they both may nevertheless contain different and valuable information about the high resolution portion of $\mathbf{m}$. In that case neither of them should be discarded of. In the following we suggest a systematic and unique approach preserving this valuable information.

An error $\delta\mathbf{m}$ of a measurement induces an error $\delta\mathbf{s}$ that can be estimated from

$$|\delta\mathbf{s}| \leqslant \frac{1}{\sqrt{\lambda_{N_c}}}|\delta\mathbf{m}|. \tag{3}$$

Here λ_{N_c} is the smallest eigenvalue of the positive definite matrix $\mathcal{S}^+\mathcal{S}$. ($\lambda_{N_c} = 0$ can be excluded because otherwise $\mathbf{s}$ could not be determined and tomography would fail anyway.) Next we define densities by putting weights $a_{\nu|\mathbf{x}_l}$ on the measuring points as

$$\rho_\nu(\mathbf{x}) = \sum_{l=1}^{N_H} \frac{a_{\nu|\mathbf{x}_l}}{N_H} \cdot \delta(\mathbf{x} - \mathbf{x}_l), \qquad \int d\mathbf{x}\, \rho_\nu(\mathbf{x}) = 1. \tag{4}$$

The mathematical meaning of the densities ρ_ν will become clear below. The physical idea is the following: Imagine that in the close neighborhood of point $\mathbf{x}_k$ many (n_k) measurements are taken. These can be summed up by giving a weight n_k to the point $\mathbf{x}_k$. At the end the normalization will lead to the weight a_k of that point.

We obtain for a distribution of measuring points, ρ_ν, the matrix

$$D_{\nu|i,j} = \int d\mathbf{x}\, S^+_{i,\mathbf{x}} \rho_\nu(\mathbf{x}) S_{\mathbf{x},j} \tag{5}$$

($\rho_\nu(\mathbf{x})$ has to be normalized to exclude multiplication of $\mathcal{D}_\nu$ with a simple factor).

To minimize the absolute error, we iterate $\rho_\nu(\mathbf{x})$ such that the smallest eigenvalue of $\mathcal{D}_\nu$, $\lambda_{\nu|N_c}$, is maximized. At the beginning we choose a density ρ_0 with e.g. equal weight of all $a_{0|i}$. Then we iterate in the following manner

$$\rho_\nu(\mathbf{x}) = \rho_{\nu-1}(\mathbf{x}) \cdot \big(1 + \epsilon_\nu \tau_\nu(\mathbf{x})\big), \tag{6}$$

$\epsilon_\nu\tau_\nu$ is a small relative change of the density. Using the density $\rho_{\nu-1}$ for normalizing τ_ν, and keeping in mind the condition $\int \rho_i = 1$ for all i, we obtain the constraints

$$\int d\mathbf{x}\, \rho_{\nu-1}(\mathbf{x}) \cdot \tau_\nu^2(\mathbf{x}) = 1,$$
$$\int \rho_\nu - \int \rho_{\nu-1} = 0, \quad \text{or} \quad \int d\mathbf{x}\, \rho_{\nu-1}(\mathbf{x}) \cdot \tau_\nu(\mathbf{x}) = 0. \tag{7}$$

We denote with $\mathcal{T}_\nu$ the unitary transformation diagonalizing $\mathcal{D}_{\nu-1}$ and suppose that the lowest eigenvalue of $\mathcal{D}_{\nu-1}$, $\lambda_{\nu-1|N_c}$ is N_η fold degenerate or nearly degenerate. Then τ_ν is chosen such that the center of mass of these N_η eigenvalues, $\mu_{\nu-1|\lambda}$ increases i.e. $\mu_{\nu-1} < \mu_\nu$. (This procedure includes the nondegenerate case, $N_\eta = 1$.) We define the quantity $d_{\nu|1}$

$$d_{\nu|1}(\mathbf{x}_k) = \frac{1}{N_\eta} \sum_{i=N_C-N_\eta+1}^{N_C} \left| \sum_l S_{\mathbf{x}_k,l} T_{\nu|l,i} \right|^2. \tag{8}$$

In first order perturbation theory (i.e. in linear approximation) the change of $\mu_{\nu-1}$ is given by:

$$\mu_\nu - \mu_{\nu-1} = \epsilon_\nu \int d\mathbf{x}\, d_{\nu|1}(\mathbf{x})\, \rho_{\nu-1}(\mathbf{x}) \tau_\nu(\mathbf{x}) + \mathcal{O}\big(\epsilon_\nu^2\big). \tag{9}$$

It follows from (7) and (9) that τ_ν can be expanded uniquely as

$$\tau_\nu(\mathbf{x}) = \sum_{m=1}^{2} \alpha_m\, d_{\nu|m}(\mathbf{x}), \quad d_{\nu|2}(\mathbf{x}) = const. \tag{10}$$

Introducing the matrix

$$X_{\nu|i,j} = \int d\mathbf{x}\, d_{\nu|i}(\mathbf{x})\, \rho_{\nu-1}(\mathbf{x})\, d_{\nu|j}(\mathbf{x}), \tag{11}$$

the change of $\mu_{\nu-1}$ can be expressed by

$$\mu_\nu - \mu_{\nu-1} = \epsilon_\nu \sum_{l=1}^{2} X_{\nu|1,l}\alpha_l, \tag{12}$$

with the constraints due to (7)

$$\sum_{l=1}^{2} X_{\nu|2,l}\alpha_l = 0, \qquad \sum_{l,l'=1}^{2} \alpha_l X_{\nu|l,l'}\alpha_{l'} = 1. \tag{13}$$

From these equations the optimum τ_ν can be found by maximizing the functional

$$F_\nu(\boldsymbol{\alpha}) = \sum_{l=1}^{2} X_{\nu|1,l}\alpha_l - \kappa_0 \sum_{l=1}^{2} X_{\nu|2,l}\alpha_l - \kappa_1 \sum_{l,l'}^{2} \alpha_l X_{\nu|l,l'}\alpha_{l'}. \tag{14}$$

Here the first sum contains the change of $\mu_{\nu-1}$ in first order perturbation theory. The second and third sum take care of the constraints, cf. (13). κ_0 and κ_1 are Lagrange parameters to be inserted such that the constraints are fulfilled. Because of the orthogonality constraint in (7), the correction function τ_ν changes sign. Thus there is a maximal iteration strength $\epsilon_{\max} > 0$ with

$$\epsilon_{\max} = \max_\epsilon \big\{1 - \epsilon\, \tau_\nu(\mathbf{x}) \geqslant 0, \ \text{for all } \mathbf{x}\big\}, \tag{15}$$

and we select e.g. $\epsilon_\nu = 0.5\epsilon_{\max}$.

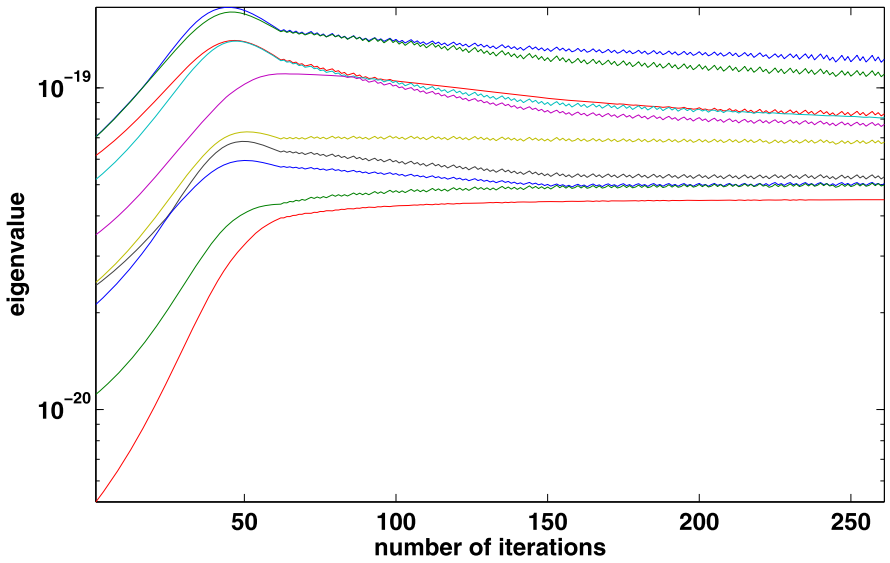

Fig. 1. Shown are the 10 lowest eigenvalues of the matrix $\mathcal{D}_\nu$ in the magnetotomographic problem during iterations ν as described in the text. Note the steep rising of the lowest eigenvalue $\lambda_{\nu|N_c}$ by a factor of 8.7.

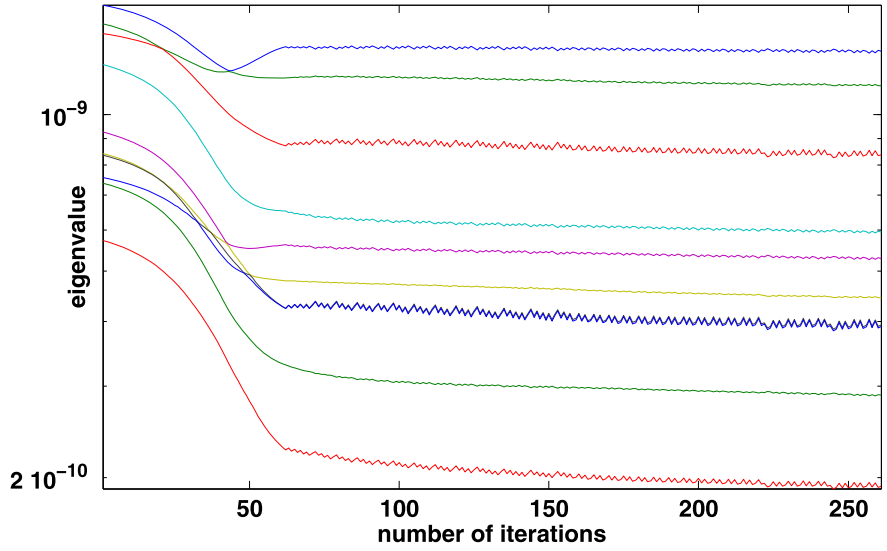

Fig. 2. Shown are the 10 largest eigenvalues of the matrix $\mathcal{D}_\nu$ in the magnetotomographic problem during iterations ν as described in the text. In contrast to the lowest eigenvalue the highest eigenvalue does not change very much since the optimization procedure does not take care of it.

The described iteration is repeated till the lowest eigenvalue $\lambda_{\nu|N_c}$ of $\mathcal{D}_\nu$ does no longer increase. We denote the obtained density by ρ_∞, the obtained matrix by $\mathcal{D}_\infty$ and its eigenvalues by $\lambda_{\infty|i}$. Then we solve instead of (2) the equation

$$\sqrt{\rho_\infty}\mathbf{m} = \sqrt{\rho_\infty}\mathcal{S}\mathbf{s} \tag{16}$$

($(\sqrt{\rho_\infty}\mathbf{m})_k$ is a symbolic notation for $\sqrt{a_{\infty|k}/N_H}m_k$, etc.). The absolute error of a measuring device does not depend on position and therefore because of (4)

$$|\delta\mathbf{m}| \approx |\sqrt{\rho_\infty}\delta\mathbf{m}|, \tag{17}$$

and consequently (3) is replaced by

$$|\delta\mathbf{s}| \leqslant \frac{1}{\sqrt{\lambda_{\infty|N_c}}}|\delta\mathbf{m}|, \quad \lambda_{\infty|N_c} > \lambda_{N_c}, \tag{18}$$

which means that the absolute error of $\delta\mathbf{s}$ has been reduced.

But we can do much better than that. The process of the iterative optimization produces most likely a very inhomogeneous density $\rho_\infty(\mathbf{x})$. Some measuring points get a very high weight, the weight of other positions becomes negligible. This is very important because in this way measuring points are labeled as irrelevant. So after a successful iterative optimization it is consistent to cut out measuring points with low weight. This is easily done by admitting only positions with weight larger than some a_{XO}. Let us assume that after removal of the measuring points having small weight the first $\breve{N}$ measuring points remain. Then we get $\breve{\mathbf{m}}$ by removing in $\mathbf{m}$ all components $i > \breve{N}$, $\breve{\mathcal{S}}$ by removing in $\mathcal{S}$ all lines $i > \breve{N}$ and $\breve{\rho}$ by replacing N_H in (4) with $\breve{N}$ and multiplying the sum with an appropriate factor to get the normalization right. After applying the optimization procedure again for the reduced set of $\breve{N}$ measuring points we have to solve (using the corresponding notations $\breve{\rho}_\infty$, $\breve{\mathcal{D}}_\infty$ and $\breve{\lambda}_{\infty|N_c}$)

$$\sqrt{\breve{\rho}_\infty}\breve{\mathbf{m}} = \sqrt{\breve{\rho}_\infty}\breve{\mathcal{S}}\mathbf{s}. \tag{19}$$

The error estimate is now

$$|\delta\mathbf{m}| \approx |\sqrt{\rho_\infty}\delta\mathbf{m}| \approx |\sqrt{\breve{\rho}_\infty}\delta\mathbf{m}| \geqslant \sqrt{\breve{\lambda}_{\infty|N_c}}|\delta\mathbf{s}|, \tag{20}$$

$$\check{\lambda}_{\infty|N_c} \approx \lambda_{\infty|N_c}. \tag{21}$$

Because only the irrelevant measuring points are discarded, it is expected, that the eigenvalue spectra of $\mathcal{D}_\infty$ and $\check{\mathcal{D}}_\infty$ essentially agree. This is indeed the case as can be seen from the example in the next section justifying the above relation $\check{\lambda}_{\infty|N_c} \approx \lambda_{\infty|N_c}$. Thus (20) demonstrates the effect that *both*, the absolute error $|\delta\mathbf{s}|$ *and* the number of measuring points N_H can be reduced by our method. Of course, established tomographic procedures have been optimized already using other methods, and there this effect is possibly not significant. On the other hand our procedure gives a systematic approach to choosing the best distribution of measuring points. That the resulting effect can be rather dramatic, will be shown in the next section for a realistic problem of magnetotomography.

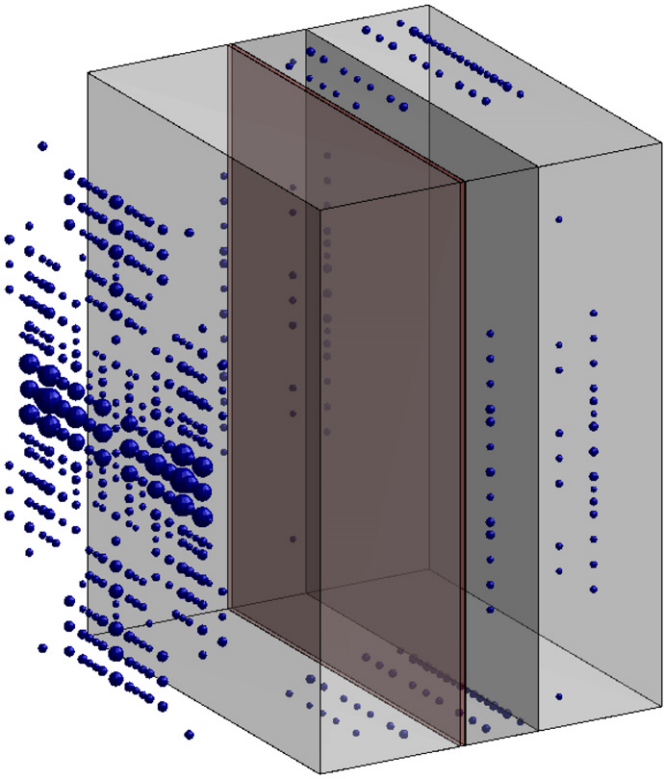

Fig. 3. The distribution of measuring points at the end of the second optimization run in the magnetotomographic problem of an experimental fuel cell (cross section 138×178 mm^2, thickness ≈ 4 cm). The dark [magenta in the web version] shaded layer is the MEA (thickness ≈ 0.5 mm). The size of the spheres corresponds to the weight of the measuring points. Their number, originally 6702, is reduced to 498.

3. An example: magnetotomography of fuel cells

To show the power of our novel optimization procedure we have applied it to magnetotomography by doing numerical computations for a realistic model of a fuel cell.

Magnetotomography can supply valuable information about the specific effective conductivity $\sigma_{\mathrm{MEA}}(\mathbf{r})$ in the heart of the low temperature fuel cell, the **M**embrane **E**lectrode **A**ssembly (MEA). The reason is that i) the currents are rather large in a fuel cell, ii) except for the MEA all specific conductivities in the fuel cell are known and therefore the current distribution $\mathbf{j}$ in the whole fuel cell depends uniquely on $\sigma_{\mathrm{MEA}}(\mathbf{r})$. Furthermore the external magnetic field is uniquely determined by the internal currents of the fuel cell (in the simplest case by the Biot–Savart integral formula [13]). The magnetic field measurements at various positions are collected in the vector $\tilde{\mathbf{m}} \in \hat{V}$. The dimension of $\hat{V}$ is three times the number of measuring points. The coefficients of an appropriately normalized basis of $\sigma_{\mathrm{MEA}}(\mathbf{r})$ are the components of $\tilde{\mathbf{s}} \in V$. The dimension of V depends on the resolution required for $\sigma_{\mathrm{MEA}}(\mathbf{r})$. From the properties stated above follows that $\tilde{\mathbf{m}}$ is uniquely determined by $\tilde{\mathbf{s}}$ and thus (1) holds true. Let the deviations from the operating point be $\mathbf{m}$ and $\mathbf{s}$ respectively. Then it is a tedious but in principle straightforward task to compute the linear relation between $\mathbf{m}$ and $\mathbf{s}$ leading to (2). The linear approximation is very good in this case [22,23]. Moreover we know that magnetotomography is unique [28], therefore the matrix $\mathcal{S}^+\mathcal{S}$ is positive definite.

The measuring points are positioned in 6 planes 1 cm above each surface of the fuel cell. The distribution of measuring points

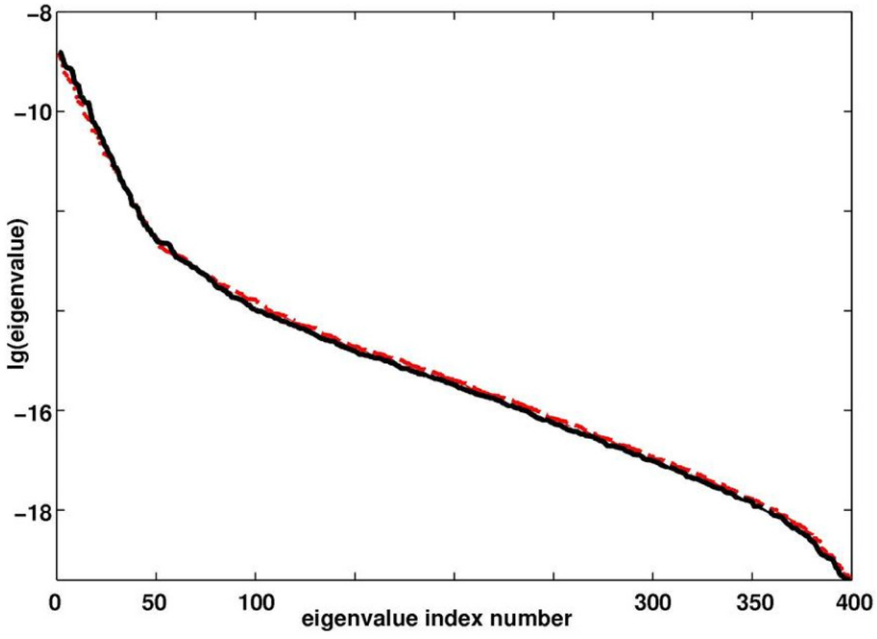

Fig. 4. Comparison of the eigenvalue spectrum obtained from $\mathcal{D}_\infty$ at the end of the first optimization run ([red in the web version] dashed line) with the eigenvalue spectrum obtained from $\check{\mathcal{D}}_\infty$ at the end of the second optimization run (black full line) in the magnetotomographic problem.

is initially homogeneous, similar to that chosen in [14] and consisting of 6702 (4 mm distance to each next neighbor) measuring points. The dimension of V is 399. This corresponds to 400 conductivities on a 2 dimensional grid (a 3 dimensional grid was not necessary since the MEA in a fuel cell is typically very thin, 0.5 mm or less). Further details about the arrangement, the numerics and a heuristic method for finding the relevant measuring points are given in [12].

Applying the scheme described above the optimal density distribution is obtained after about 150 iterations. In our case the iteration was stopped after the lowest eigenvalue of $\mathcal{D}_\nu$ did not increase any more. This was the case after 260 iterations.

In Fig. 1 and Fig. 2 it is shown how the eigenvalues change during the first optimization procedure. While the lowest eigenvalue rises by a factor of about 9, which is equal to an enhancement of the absolute precision by a factor of 3, the highest eigenvalues are nearly constant. Due to the relation of the highest to the lowest eigenvalue, the relative precision has increased by a factor of 3.5.

Next all measuring points with the smallest weights, in our case weights less than $a_{XO} = 1$, are discarded. In this way one gets rid of more than 90% of the measuring points and only 498 measuring points remain.

After the elimination of the irrelevant measuring points the same optimization procedure as before is applied, but now varying the density represented by the remaining 498 measuring points. The optimized density of the remaining measuring points is shown in Fig. 3. As expected also from Fig. 4 the precision obtained with the remaining measuring points is nearly the same as before. We gain a factor of 2.7 for the absolute precision and a factor of 3.3 for the relative precision.

4. Conclusion

In this Letter we have shown: Even if measurements are done very carefully at every position, their relevance can be quite different in tomographic problems. We have suggested a novel procedure how by detecting the relevant and by eliminating the irrelevant measuring points the precision of the tomographic reconstruction can be increased. In our numerical example of magnetotomography the elimination is rather drastic, the number of measuring points is reduced by more than 90%, nevertheless the precision (absolute and relative) of the tomographic reconstruction increases by a factor of about 3.

Modifying the optimization described here is possible, e.g. direct minimization of relative errors or taking into account that at some measuring points measurements are more difficult and should be avoided if possible. This will be described in more detail in a forthcoming article.

References

[1] F. Natterer, The Mathematics of Computerized Tomography, B.G. Teubner, Stuttgart, 1986.
[2] A.C. Kak, M. Slaney, Principles of Computerized Tomographic Imaging, IEEE Press, New York, 1988.
[3] R. Xia, X. Li, B. He, IEEE Trans. Biomed. Eng. 57 (2010) 708.
[4] R. Duwe, P. Jansen, Nucl. Eng. Des. 130 (1991) 89.
[5] M.M. Ter-Pogossian, M.E. Phelps, E.J. Hoffmann, N.A. Mullani, Radiology 114 (1975) 89.
[6] H. Young, et al., Eur. J. Cancer 35 (1999) 1773.
[7] H.W.E. Klunk, et al., Ann. Neurol. 55 (2004) 306.
[8] D. Isaacson, IEEE Trans. Med. Im. MI-5 (1986) 91.
[9] K. Paulson, W. Lionheart, M. Pidcock, IEEE Trans. Med. Im. 12 (1993) 681.
[10] A.F. Frangi, P.J. Riu, J. Rosell, M.A. Viergever, IEEE Trans. Med. Im. 21 (2002) 566.
[11] X. Li, Y. Xu, B. He, IEEE Trans. Biomed. Eng. 54 (2007) 323.
[12] H. Lustfeld, M. Reißel, U. Schmidt, B. Steffen, J. Fuel Cell Sci. Technol. 6 (2009) 021012.
[13] R. Kress, L. Kühn, R. Potthast, Inverse Problems 18 (2002) 1127.
[14] K.-H. Hauer, R. Potthast, T. Wüster, D. Stolten, J. Power Sources 143 (2005) 67.
[15] Y. Xu, O. Tischenko, C. Hoeschen, SIAM J. Numer. Anal. 45 (2007) 108.
[16] A. Kemna, Tomographic Inversion of Complex Resistivity, Der andere Verlag, Osnabrueck, 2000.
[17] D. Khosla, M. Singh, IEEE Trans. Nucl. Sci. 44 (1997) 1368.
[18] M. Freiberger, H. Scharfetter, Proc. of SPIE 7174 (2009) 717419.
[19] Y. Xu, O. Tischenko, C. Hoeschen, Proc. of SPIE 6142 (2006) 61422A.
[20] O. Tischenko, Y. Xu, C. Hoeschen, Proc. of SPIE 6142 (2006) 61422L.
[21] Y. Xu, O. Tischenko, East J. Approx. 13 (2007) 427.
[22] J.A. Hirschfeld, Jül-Report Jül-4291, Forschungszentrum Jülich, http://hdl.handle.net/2128/3588, 2009.
[23] H. Lustfeld, M. Reißel, B. Steffen, Fuel Cells 9 (2009) 474.
[24] C.L. Lawson, R.J. Hanson, Solving Least Squares Problems, SIAM, Philadelphia, 1995.
[25] A.J. Appleby, F.R. Foulkes, Fuel Cell Handbook, van Nostrand Reinhold, New York, 1988.
[26] Y.-G. Yoon, W.-Y. Lee, T.-H. Yang, G.-G. Park, C.-S. Kim, J. Power Sources 118 (2003) 193.
[27] A. Curtis, A. Michelini, D. Leslie, A. Lomax, Geophys. J. Int. 157 (2004) 595.
[28] H. Lustfeld, J.A. Hirschfeld, M. Reißel, B. Steffen, J. Phys. A 42 (2009) 495205.